IOPscience iopscience.iop.org

Home Search Collections Journals About Contact us My IOPscience

Characteristics of deep levels in n-type CdTe

This article has been downloaded from IOPscience. Please scroll down to see the full text article.

1991 J. Phys.: Condens. Matter 3 8619

(http://iopscience.iop.org/0953-8984/3/44/008)

View the table of contents for this issue, or go to the journal homepage for more

Download details:
IP Address: 171.66.16.159
The article was downloaded on 12/05/2010 at 10:41

Please note that terms and conditions apply.

J. Phys.: Condens. Matter 3 (1991) 8619–8634. Printed in the UK

Characteristics of deep levels in n-type CdTe

G M Khattak and C G Scott
Department of Applied Physics, University of Hull, Hull HU6 7RX, UK

Received 20 May 1991

Abstract. Deep-level transient spectroscopy has been employed to study the defect states in n-type CdTe crystals subjected to a variety of annealing treatments. By comparing the results from crystals grown by the Bridgman and travelling heater methods (starting from a common source of CdTe) and by considering the variation in properties with position along each boule, it was concluded that the electrical properties were strongly influenced by residual impurities in these materials. Eleven different defect states were detected with activation energies ranging from 0.2 eV to 0.86 eV. One of these was found only in In-doped samples and at least three were related to residual impurities and could be removed by annealing in liquid cadmium. Several defects were interpreted as complex centres involving native defects and impurities.

1. Introduction

Although CdTe is unique amongst the wide-bandgap II–VI compounds in being the only member of this group that can be easily made in both p-type and n-type forms, progress towards its exploitation in a wide and diverse range of potential devices has been rather slow due to problems associated with the reliable preparation of crystals with the required size, purity and crystal quality. Lack of control over the defect structure of these materials has affected development of a satisfactory understanding of the nature and behaviour of the defects that act as traps or recombination centres and control the electrical properties of the material.

Although the early work of de Noble [1], Kroger [2] and others was interpreted mainly in terms of native defects, it is now known that residual impurities can play a dominating role, but there is clearly a need to identify all the various defect states that arise in CdTe and to determine the associated trapping characteristics. In the last decade, the results of several investigations of defect levels in CdTe have been reported [3–8], but while these reports reveal the presence of some commonly occurring traps, as discussed in section 4 below, there are also many inconsistencies which are difficult to explain in the absence of sufficiently detailed information about the crystal quality and purity of the different samples studied. For example, in a previous study in this laboratory [9] results were obtained for samples produced by two different growth techniques (the Bridgman method and the travelling heater method (THM)). These two sets of samples were found to have significantly different properties even after high-temperature annealing under identical conditions. However, it was not possible to associate these differences simply with the different growth methods because the two sets of samples

0953-8984/91/448619 + 16 $03.50 © 1991 IOP Publishing Ltd

were grown in different laboratories and the source materials would be expected to contain different residual impurities. In order to explore this problem a further experiment has now been conducted in which the two different growth methods have again been employed but, in this case, identical material was used as the source. The results indicate significant differences between the Bridgman- and THM-grown samples and by studying the effects of different post-growth treatments, a number of traps related to residual impurities have been identified.

2. Experimental details

2.1. Sample preparation

The initial common source of CdTe was produced from a stoichiometric mix of high-purity (6N) cadmium and tellurium. This was split into two equal parts and each half was separately regrown in the form of a 15 mm diameter boule using the Bridgman method and one of these boules was subsequently regrown by THM using Te as the solvent. Each boule was sliced into a set of discs with thickness of about 2 mm and these discs were subsequently cut into segments, each with an area of approximately 5 mm × 5 mm. Samples cut from Bridgman-grown boules are designated by the letter B in the results presented below while samples grown by THM are designated by the letter T. The sample number indicates the position of the associated disc within the original boule (starting with disc number one at the bottom of each boule).

The CdTe crystals grown by both the above techniques were found to be p-type. As it is difficult to form reliable ohmic contacts to p-type material, all the samples studied here were first converted to n-type by annealing for various lengths of time at 800 °C under saturated Cd pressure. Some samples were doped with In during the annealing process.

2.2. Characterization techniques

Measurements of the free-carrier concentration were made using both the Hall effect and the capacitance–voltage (C–V) method. Hall effect measurements were performed using the Van der Pauw [10] technique. The ohmic contacts for this were achieved by soldering with In. For the capacitance–voltage measurements Schottky diodes were produced by evaporating dots of Au and In, of 1 mm and 2 mm diameter, onto opposite faces of the samples to provide Schottky and ohmic contacts, respectively. These same Schottky diodes were employed for characterization of the trapping states using the deep-level transient spectroscopy (DLTS) technique. These measurements were made using the double boxcar method, as described by Lang [11], incorporating a Boonton capacitance meter (Model 72B). With gate opening times t_1 and t_2, the emission rate window, e_n, can be expressed as [11]

$$e_n = \ln(t_1/t_2)/(t_1 - t_2) \tag{1}$$

and this was corrected for the time constant of the capacitance meter [12]. Trap concentrations N_T were calculated from [13]:

$$N_T = \frac{2n\,\Delta C_0}{C(V)}\left[1 - \frac{2\lambda}{W(V)}\left(1 - \frac{C(V)}{C(0)}\right) - \left(\frac{C(V)}{C(0)}\right)^2\right]^{-1} \tag{2}$$

where n is the free-electron concentration, ΔC_0 is the capacitance at the end of the filling pulse, $W(V)$ is the depletion layer width at reverse bias V, $C(0)$ and $C(V)$ are the steady-state capacitances at zero and reverse bias V, respectively and λ is the width of the edge region defined by [14].

$$\lambda = 2\varepsilon\varepsilon_0(E_F - E_T)/q^2 n \tag{3}$$

where E_T is the trap depth from the conduction band and the other symbols have their usual meaning. The activation energy E_T and the apparent electron capture cross-section σ_n were calculated from

$$e_n = N_C V_{th} \sigma_n \, e^{-E_T/kT} \tag{4}$$

where N_C ($= 1.44 \times 10^{14}\, T^{3/2}\, cm^{-3}$) and V_{th} ($= 2.18 \times 10^6\, T^{1/2}\, cm\, s^{-1}$) are the conduction band density of states and mean thermal speed of the free electrons respectively.

3. Results

3.1. Carrier concentration measurements

Table 1 shows the measured values for free-carrier concentration in B and T samples which had all been annealed for 48 hours. The values calculated from Hall effect and *C–V* measurements are seen to be in reasonable agreement with each other and it is clear from these results that the variations in carrier concentration values follow a trend such that the samples that were prepared from slices in the lower sections of the boules (e.g. B4.1 and T2.1) have higher values than for those from slices near the top (e.g. B32 and T35). Table 2 shows the effect of shorter and longer annealing times on the carrier concentration for samples from a particular slice (in comparison with 48 h annealing). Samples B4.2, T2.2 and samples B4.3 and T2.3 were annealed for one hour and one week respectively. It is clear from table 2 that the carrier concentration increases with longer annealing times as reported by de Noble [1].

In order to compare the results of the present work with previously published DLTS data [9] additional periods of annealing (40 and 91 h) were employed with and without

Table 1. Electrical characteristics of samples annealed for 48 h at 800 °C under saturated cadmium pressure.

	Free carrier concentration at room temperature obtained from	
Sample number†	Hall measurement (cm^{-3})	*C–V* measurement (cm^{-3})
B4.1	2.78×10^{16}	2.65×10^{16}
B20	1.01×10^{16}	1.24×10^{16}
B32	7.45×10^{15}	7.49×10^{15}
T2.1	7.86×10^{16}	8.10×10^{16}
T21	1.16×10^{16}	1.87×10^{16}
T35	8.83×10^{15}	8.03×10^{15}

† Slices grown by Bridgman method (B) = 1 (bottom) to 41 (top). Slices grown by THM (T) = 1 (bottom) to 45 (top).

Table 2. Carrier concentration for samples annealed for different lengths of time.

Sample number†	Anneal time	Free carrier concentration obtained from C–V measurement at room temperature (cm^{-3})
B4.2	1 h	7.72×10^{15}
B4.1	48 h	2.65×10^{16}
B4.3	1 wk	1.93×10^{17}
T2.2	1 h	7.87×10^{15}
T2.1	48 h	8.00×10^{16}
T2.3	1 wk	2.06×10^{17}

† Slices grown by Bridgman method (B) = 1 (bottom) to 41 (top). Slices grown by THM (T) = 1 (bottom) to 45 (top).

doping. Table 3 shows the carrier concentration at room temperature for all the undoped and In-doped samples used in this study. It is interesting to note from the results in tables 1, 2 and 3 that the values of carrier concentration in the T samples were always slightly higher than those of the B samples (after firing under similar conditions).

3.2. DLTS measurements

DLTS spectra for two nominally undoped samples (B2 and T3) after 48 h treatment are shown in figure 1. Six peaks labelled EB1, EB2, EB4, EB5, EB6 and EB7 in sample B2 and five peaks labelled ET2, ET4, ET5, ET6 and ET7 in sample T3 can be seen within the range 77 to 400 K.

Figure 2 shows results for a second set of samples (B30.1 and T37.1) which were annealed for 40 h with In present. Six deep levels are again observed in the B sample (Sample B30.1) but the feature EB4 is seen to be replaced by EB3. For the T sample (Sample T37.1) the new features are ET1 and ET3 while ET4 is absent.

To study the effect of different annealing times, two samples B30.2 and T37.2 (from the same slices as the samples B30.1 and T37.1) were annealed (with In present) for 91 h instead of 40 h. The resulting DLTS spectrum for sample B30.2 showed the same peaks as observed in sample B30.1. For sample T37.2 the trap ET4 was seen once again in place of ET3 but a peak which appeared at the same temperature as the previous ET2 feature was found to have very different properties to ET2 as discussed later. This new feature has been designated ET2a.

Table 3. Electrical characteristics of samples used for DLTS studies.

Sample number	Annealing conditions	Free carrier concentration at room temperature (cm^{-3})
B2	48 h (undoped)	4.49×10^{16}
B30.1	40 h (In doped)	5.77×10^{15}
B30.2	91 h (In doped)	4.72×10^{16}
T3	48 h (undoped)	7.49×10^{16}
T37.1	40 h (In doped)	7.86×10^{15}
T37.2	91 h (In doped)	7.86×10^{16}

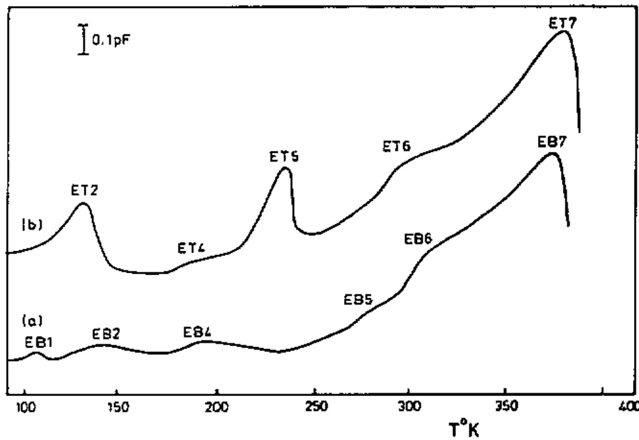

Figure 1. DLTS spectra for two undoped samples using a rate window of 162 s^{-1}. Curve (*a*) for sample B2 and curve (*b*) for sample T3.

Arrhenius plots of e_n/T_m^2 versus $10^3/T_m$, where T_m is the temperature of the DLTS peak maximum, for all the electron traps (except ET2a) detected in the above B and T samples are presented in figure 3. Tables 4 and 5 give the thermal activation energies E, trap concentrations N and apparent electron capture cross-sections σ_n for all these traps as calculated using equations (2) and (4). The symbol '0' in these tables indicates that a peak was detected but the amplitude was too small for an accurate analysis to be carried out.

3.3. *Temperature dependence of electron capture cross-section*

The activation energies given in tables 4 and 5 were obtained under the assumption that the capture cross-section σ_n is independent of temperature. Furthermore, the use of

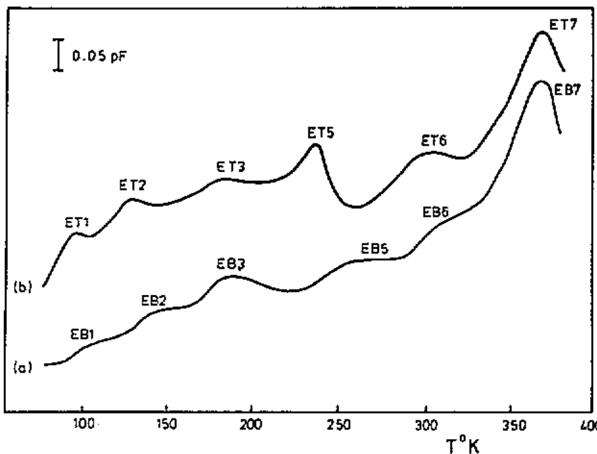

Figure 2. DLTS spectra for two In-doped samples (rate window 95.2 s^{-1}). Curve (*a*) sample B30.1 and curve (*b*) sample T37.1.

Table 4. Measured trap parameters for CdTe samples grown by the Bridgman method, after various anneal treatments.

Sample number	Annealing conditions	Trap parameters	Trap						
			EB1	EB2	EB3	EB4	EB5	EB6	EB7
B2	48 h (undoped)	E_T (eV)	0.21 ± 0.02	0.38 ± 0.03	—	0.24 ± 0.01	0	0	0.86 ± 0.02
		N_T (cm^{-3})	1.04×10^{13}	1.53×10^{13}	—	1.6×10^{13}	$\sim 10^{13}$	$\sim 10^{13}$	1.26×10^{14}
		σ_n (cm^2)	4.57×10^{-14}	1.28×10^{-9}	—	2.42×10^{-17}	—	—	1.70×10^{-12}
B30.1	40 h (In-doped)	E_T (eV)	0.20 ± 0.02	0.38 ± 0.02	0.34 ± 0.01	—	0.58 ± 0.03	0.69 ± 0.04	0.86 ± 0.03
		N_T (cm^{-3})	5.25×10^{12}	9.09×10^{12}	9.19×10^{12}	—	9.22×10^{12}	2.09×10^{13}	1.05×10^{14}
		σ_n (cm^2)	1.22×10^{-14}	1.98×10^{-9}	1.27×10^{-13}	—	2.26×10^{-15}	2.99×10^{-13}	1.54×10^{-12}
B30.2	91 h (In-doped)	E_T (eV)	0.21 ± 0.01	0.39 ± 0.03	0.34 ± 0.01	—	0.60 ± 0.04	0.69 ± 0.01	0.86 ± 04
		N_T (cm^{-3})	1.26×10^{13}	2.46×10^{13}	2.69×10^{13}	—	3.55×10^{13}	6.46×10^{13}	2.71×10^{14}
		σ_n (cm^2)	5.28×10^{-14}	2.72×10^{-9}	2.76×10^{-13}	—	3.34×10^{-15}	3.06×10^{-13}	1.71×10^{-12}

Table 5. Measured trap parameters for CdTe samples grown by the THM, after various anneal treatments.

Sample number	Annealing conditions	Trap parameters	Trap							
			ET1	ET2	ET2a	ET3	ET4	ET5	ET6	ET7
T3	48 h (Un-doped)	E_T (eV)	—	0.28 ± 0.01	—	—	0.24 ± 0.01	0.46 ± 0.02	0	0.86 ± 0.02
		N_T (cm^{-3})	—	2.44×10^{13}	—	—	1.64×10^{13}	3.00×10^{14}	$\sim 10^{14}$	6.7×10^{14}
		σ_n (cm^2)	—	6.48×10^{-13}	—	—	5.74×10^{-17}	7.72×10^{-14}	—	2.07×10^{-12}
T37.1	40 h (In-doped)	E_T (eV)	0.22 ± 0.02	0.28 ± 0.02	—	0.34 ± 0.01	—	0.46 ± 0.02	0.68 ± 0.01	0.86 ± 0.03
		N_T (cm^{-3})	6.15×10^{12}	2.27×10^{13}	—	2.65×10^{13}	—	4.92×10^{13}	4.05×10^{13}	3.9×10^{14}
		σ_n (cm^2)	8.62×10^{-13}	3.44×10^{-13}	—	5.48×10^{-13}	—	2.55×10^{-14}	2.43×10^{-13}	1.77×10^{-12}
T37.2	91 h (In-doped)	E_T (eV)	0.21 ± 0.01	—	0.06	—	0.24 ± 0.03	0.45 ± 0.02	0.69 ± 0.03	0.86 ± 0.01
		N_T (cm^{-3})	2.35×10^{13}	—	6.85×10^{13}	—	2.67×10^{13}	5.18×10^{14}	7.02×10^{14}	9.4×10^{14}
		σ_n (cm^2)	7.83×10^{-13}	—	—	—	4.27×10^{-17}	3.74×10^{-14}	3.0×10^{-13}	2.08×10^{-12}

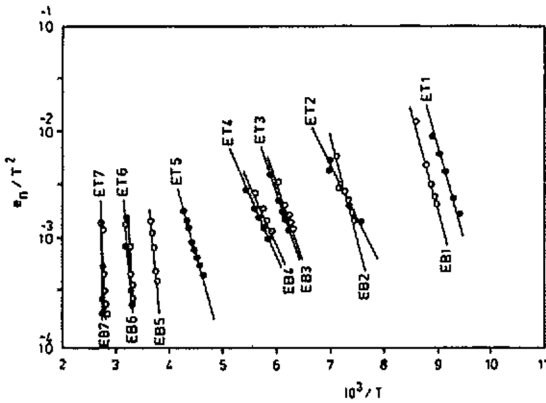

Figure 3. Emission rate data for traps listed in tables 4 and 5. ○ denotes B samples, ● denotes T samples.

equation (4) to derive values of σ_n from Arrhenius plots implicitly assumes that the entropy change $\Delta S = 0$ for the reaction (4), so σ_n values calculated in this way represent upper limits for these parameters. However, it follows that ΔS can be evaluated if σ_n can be measured directly. This can be done by observing how the DLTS peak amplitude changes with the width of the filling pulse, since the peak height is proportional to the number of filled traps. Of course, this requires the use of filling pulse times that are sufficiently short to avoid total filling of the traps. In this study, using filling pulses from 100 ms down to 1 ms, a significant change in peak height was observed only for the feature designated ET2a, indicating that all the other traps were completely filled in less than 1 ms.

A plot of the variation in the magnitude ΔC_0 of the DLTS peak with filling pulse width t_f, for the trap ET2a, is shown in figure 4. The trap filling is expected to proceed according to

$$\mathrm{d}N(t)/\mathrm{d}t = e_n N(t) - c_n n(N_T - N(t)) \quad (5)$$

where $c_n = \sigma_n v_{th}$, N_T is the total trap concentration and $N(t)$ is the concentration of

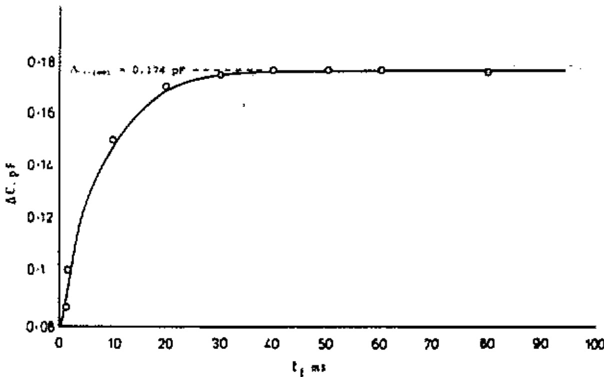

Figure 4. Variation of DLTS peak amplitude ΔC_0 with filling pulse width t_f for trap ET2a.

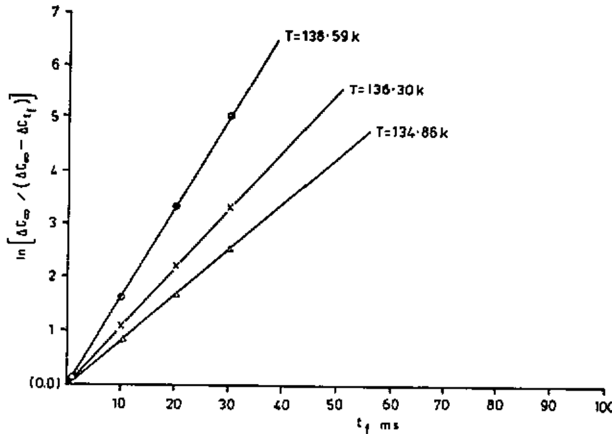

Figure 5. Dependence of DLTS peak amplitude on filling pulse width for three different rate windows corresponding to three different peak temperatures.

occupied traps at time t. The solution of equation (5) for $N(t)$ initially zero is

$$N(t) = [c_n n N_T/(c_n n + e_n)][1 - \exp(-(c_n n + e_n)t_f)]$$

and so the filling time constant of the traps is given by $(c_n n + e_n)^{-1}$. If $c_n n \gg e_n$ then $N(t) \rightarrow N_T$ as $t_f \rightarrow \infty$ and ΔC_m would then become independent of t_f and the rate window as observed. Figure 5 shows plots of

$$\ln[\Delta C_0(\infty)/(\Delta C_0(\infty) - \Delta C_0(t_f))]$$

versus the filling pulse duration time t_f for three different rate windows corresponding to three different temperatures. Thus, the electron capture time constant was calculated form the slope of the lines in figure 5, corresponding to the three temperatures involved. The resultant capture cross-sections (calculated assuming that $c_n n \gg e_n$) are shown in figure 6. Over this restricted temperature range, the data appear to follow a relationship of the form

$$\sigma_n = \sigma_\infty \, e^{-E_B/kT} \qquad (6)$$

where σ_∞ is the limiting value of σ_n at $T \rightarrow \infty$ and E_B is the associated activation energy [3, 15]. By substituting this relationship in equation (4) it can be seen that the energy

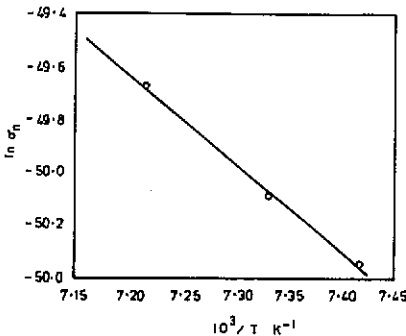

Figure 6. Electron capture cross-section versus reciprocal temperature for defect level ET2a, giving an activation energy E_B of 0.28 eV.

Table 6. Measured trap parameters for samples grown by the Bridgman method after anneal at 500 °C in Cd liquid.

Trap parameters	Trap						
	EB1	EB2	EB3	EB4	EB5	EB6	EB7
E_T (eV)	—	0.38 ± 0.02	—	0.24 ± 0.01	—	0.69 ± 0.02	0.86 ± 0.01
N_T (cm^{-3})	—	2.86×10^{13}	—	4.2×10^{13}	—	1.09×10^{14}	1.13×10^{14}
σ_n (cm^2)	—	1.98×10^{-9}	—	1.28×10^{-17}	—	1.52×10^{-13}	2.81×10^{-12}

determined from the slope of an Arrhenius plot of the kind shown in figure 3 is the sum of E_T and E_B. For the feature ET2a, this was found to be 0.34 eV. From the slope of the line in figure 6, an activation energy E_B of 0.28 eV for the capture cross-section of trap ET2a is obtained with $\sigma_\infty = 7.2 \times 10^{-12}$ cm^{-2}. Thus, it follows that the apparent true value of E_T for the trap ET2a is (0.34 − 0.28)eV = 0.06 eV. In table 5 this is the value that is given but the validity of this analysis is in doubt, as discussed more fully in section 4.

3.4. The effect of firing in liquid cadmium

In view of the assumed importance of residual impurities in CdTe, as mentioned in section 1, a further experiment was conducted using samples that were annealed in liquid Cd instead of Cd vapour. (The liquid metal treatment has been found to be successful in removing impurities from a variety of II–VI compound materials [16]). For this exercise, two samples, B30.3 and T22, were annealed at 500 °C for two weeks in liquid Cd. This resulted in carrier concentration values very similar to those for the samples annealed under Cd vapour (the values being 2.4×10^{16} and 3.0×10^{16} cm^{-3} respectively).

The DLTS spectra revealed four electron traps for each sample and the calculated trap parameters are summarized in tables 6 and 7. By comparison with the DLTS spectra in figure 1 and the almost identical parameters for corresponding peaks in the spectra for the liquid-Cd-annealed samples it appears that the same traps are present and these have been labelled accordingly. Such a comparison also indicates that the traps EB1, EB5 and ET5 that were observed in the undoped samples annealed under saturated Cd vapour were not detected in the samples annealed under Cd melt.

Table 7. Measured trap parameters for samples grown by the THM, after anneal at 500 °C in Cd liquid.

Trap parameters	Trap						
	ET1	ET2	ET3	ET4	ET5	ET6	ET7
E_T (eV)	—	0	0	—	—	0.69 ± 0.04	0.86 ± 0.04
N_T (cm^{-3})	—	$\sim 10^{13}$	—	$\sim 10^{13}$	—	1.32×10^{14}	2.27×10^{14}
σ_n (cm^2)	—	—	—	—	—	3.0×10^{-13}	3.30×10^{-12}

4. Discussion

Table 1 shows that the bottom slices of the CdTe boules have higher free-electron concentration values than those at the top, irrespective of the growth technique. In both types of sample, the bottom slices are expected to contain fewer residual impurities than the top, as the bottom of the boule crystallizes first and the concentration of residual impurities in the melt increases while the growth of the boule proceeds. For this to explain the observed variation in electron concentration throughout the boule, it must be assumed that the dominant residual impurities are those that generate acceptor states. Further improvement in purity of material during the THM growth process would then account for the uncompensated shallow donor concentrations in the T samples generally being greater than in the B samples after being annealed under identical conditions.

A general feature of both tables 1 and 2 is that the carrier concentration increases with an increase in the annealing time, irrespective of the presence of the In. High-temperature measurements of the carrier concentration (n) in undoped CdTe [17] have shown that $n \simeq 1.6 \times 10^{17}\ \mathrm{cm}^{-3}$ at 800 °C under saturated Cd pressure and this corresponds very closely with the highest values of n recorded in table 1. This evidence is consistent with native donors providing the main contribution to n in these samples, but it is clear from the DLTS measurements on samples prepared under different conditions that residual impurities play an important role in determining the overall electrical characteristics of the material. However, before considering the nature of the defects giving rise to the deep levels observed in the various samples studied, attention will be paid to those traps that were common to both types of materials (grown by the Bridgman method or by THM).

It should be noted here that in order to be able to conclude that two traps have the same origin, the calculated values for both the activation energy and the capture cross section, must be the same to within the experimental error. Thus, figure 3 and tables 4, 5, 6 and 7 indicate that traps EB3, EB4, EB6 and EB7 are identical to traps ET3, ET4, ET6 and ET7 respectively, but although the activation energy for trap EB1 is very close to that for ET1, figure 3 and the corresponding different value for σ suggest that they are not arising from the same defect. In assessing data for different samples (especially if these are reported from different laboratories) particular care is needed in comparing values of σ deduced from (4) using Arrhenius plots (as in figure 3). Clearly, the accuracy of σ is very sensitive to temperature calibration errors as has been previously recognised [18, 19] but it is unlikely that differences in σ of much more than one order of magnitude can be attributed to such errors. With this in mind consideration can now be given to determining the possible structure of the defects associated with the traps observed under the different sample preparation conditions involved in this investigation. In order to aid the interpretation of this data, comparison is made, where appropriate, with results obtained in other laboratories as tabulated in table 8.

Reference to the data in table 8 suggests that the trap EB1 is the same as that seen in a variety of different types of CdTe samples including epilayers [3, 21] as well as THM and Bridgman grown samples [9, 20, 22]. This suggests that the trap is due to a commonly occurring native defect or residual impurity. The latter seems to be the more likely explanation as the trap EB1 was not observed either in our (higher purity) THM grown samples or in our Bridgman samples which had been fired in liquid cadmium, a process which, as mentioned earlier, is expected to remove impurities [16].

Table 8 reveals that the parameters for the trap ET1 are very close to those for traps observed by other workers in both THM [8] and Bridgman grown [7] materials. Attention

Table 8. Summary of trap characteristics.

Trap	Energy (eV)	σ (cm^2)	Material type	Reference
EB1	0.21	5.28×10^{-14}	Bridgman	This work
EH1	0.22	10^{-14}	THM/In-doped	[9, 20]
EG1	0.23	10^{-14}	Bridgman	[9, 20]
E1	0.20	—	Epilayers on BaF_2	[3]
E1	0.20	1.0×10^{-15}	Epilayers on BaF_2	[21]
E1	0.21	10^{-14}	Bridgman/In-doped	[22]
ET1	0.22	8.62×10^{-13}	THM/In-doped	This work
NA1	0.23	2.8×10^{-13}	THM/In-doped	[8]
A1	0.22	3.6×10^{-13}	THM/In-doped	[8]
E2	0.22	10^{-13}	Bridgman/In-doped	[7]
EB2	0.38	2.72×10^{-9}	Bridgman	This work
EG3	0.38	—	Bridgman	[9, 20]
A4	0.38	4.9×10^{-14}	Bridgman/In-doped	[8]
E5	0.38	10^{-9}	Bridgman/In-doped	[7]
ET2	0.28	6.48×10^{-13}	THM	This work
E2	0.28	5.4×10^{-14}	Bridgman/Al-doped	[4, 23]
EH2	0.28	6.4×10^{-14}	THM	[9, 20]
E2	0.28	10^{-13}	Bridgman/In-doped	[22]
NA2	0.28	2.2×10^{-13}	Bridgman and THM/In-doped	[8]
A	0.28	1.8×10^{-13}	Bridgman and THM In-doped	[8]
E3	0.28	10^{-13}	Bridgman/In-doped	[7]
E1	0.29	—	THM	[24]
EB3	0.34	1.27×10^{-13}	Bridgman In-doped	This work
ET3	0.34	5.48×10^{-13}	THM In-doped	This work
EH3	0.34	1.4×10^{-13}	THM In-doped	[9, 20]
E3	0.34	—	Epilayers/on BaF_2	[3]
E3	0.34	6.0×10^{-14}	Epilayers/on BaF_2	[21]
E3	0.34	10^{-13}	Bridgman/In-doped	[22]
NA3	0.34	1.0×10^{-13}	THM/In-doped	[8]
E4	0.33	10^{-13}	Bridgman/In-doped	[7]
E1	0.34	—	—	[5]
EB4	0.24	2.42×10^{-17}	Bridgman	This work
ET4	0.24	5.74×10^{-17}	THM	This work
E4	0.24	—	Epilayers/on BaF_2	[3]
E4	0.24	5.0×10^{-17}	Epilayers/on BaF_2	[21]
EB5	0.58	2.26×10^{-15}	Bridgman	This work
E6	0.60	5.4×10^{-12}	Epilayers/on BaF_2	[21]
NA5	0.58	3.4×10^{-15}	THM/In-doped	[8]
A6	0.57	3.8×10^{-15}	Bridgman/In-doped	[8]
IR4	0.62	4.1×10^{-17}	—	[6]
ET5	0.46	3.74×10^{-14}	THM	This work
EH4	0.45	1.6×10^{-15}	THM	[9, 20]
E5	0.46	—	Epilayers/on BaF_2	[3]
E5	0.46	5.0×10^{-13}	Epilayers/on BaF_2	[21]
A5	0.47	1.5×10^{-15}	Bridgman and THM/In-doped	[8]
EB6	0.69	2.99×10^{-13}	Bridgman	This work
ET6	0.69	3.0×10^{-13}	THM	This work
E7	0.66	1.9×10^{-15}	Bridgman/Al-doped	[4, 23]

Table 8. Summary of trap characteristics.

Trap	Energy (eV)	σ (cm^2)	Material type	Reference
E6	0.64	—	Epilayers/on BaF_2	[3]
E4	0.65	10^{-12}	Bridgman/In-doped	[22]
A8	0.71	1.1×10^{-14}	Bridgman and THM/In-doped	[8]
E3	0.65	3.26×10^{-14}	Epilayers/on InSb	[25]
E4	0.74	2.9×10^{-14}	Epilayers/on InSb	[25]
—	0.72	—	Bridgman	[26]
EB7	0.86	1.7×10^{-12}	Bridgman	This work
ET7	0.86	2.07×10^{-12}	THM	This work
E8	0.80	3.4×10^{-14}	Bridgman/Al-doped	[4, 23]
EG6	0.84	1.8×10^{-12}	Bridgman	[9, 20]
E7	0.92	1.3×10^{-11}	Epilayers/on BaF_2	[21]
E5	0.83	10^{-8}	Bridgman/In-doped	[22]
IR5	0.85	3.8×10^{-17}	—	[6]

should also be drawn to earlier high temperature studies [27, 28] which linked an energy level at 0.2–0.4 eV below the conduction band to the presence of interstitial cadmium (Cd_i). Similarly, studies involving the thermally stimulated conductivity technique [29] revealed that traps in this region appeared most frequently in material grown at high Cd pressure. Thus, as in the present study in which all the samples were annealed under Cd, the conditions would be favourable for Cd_i formation. However, it should be noted that, in each of the cases listed in table 8, including the present study, these traps arise in In-doped samples suggesting very strongly that the traps are In related. It is interesting that these traps were not detected in our In-doped Bridgman samples but it is possible that they were present with insufficient concentration to be distinguished from the adjacent features EB1 and EB2. Further study will be necessary to clarify this point.

The trap EB2 was only observed in the Bridgman grown material and traps with a similar ionization energy (0.38 eV) have been observed by other workers [7, 8, 9, 20] also in Bridgman samples. Like EB2, the feature A4 reported by Ido *et al* [8] was found in the Bridgman grown materials subjected to a variety of different annealing conditions under Cd vapour but not in THM grown samples. They suggested that this trap was due to metallic impurities substituting for Cd. In the present case it is likely that trap EB2, is indeed, related to an impurity but in view of the very different capture cross-section values involved it is clearly not the same trap as observed by Ido *et al* [8].

Although ET2a was observed only in the THM grown material (irrespective of whether the samples were undoped or doped) traps with similar characteristics have been observed by several other workers [4, 7–9, 20, 22, 23] in both Bridgman and THM samples doped with either Al or In. In view of the common occurrence of these traps and their persistence in the more highly refined material (annealed in liquid Cd), it is believed that they must be related to native defects as has been previously suggested by Ido *et al* [8].

As noted earlier, trap ET2 was only observed in the THM material after annealing in Cd for 91 h (see table 2). This trap was unusual in having a very small and temperature-dependent capture cross-section. A very similar behaviour has been described by Takebe and co-workers (for traps arising in samples which had been annealed under a high Cd partial pressure) [4, 23] and the parameters calculated for these traps agree very well

with the results calculated here for ET2a. However, as has been pointed out by Verity *et al* [9] who also observed such features, the basis of this analysis is invalid as it depends upon the assumption that $C_n n \gg e_n$ which is inconsistent with the experimental data.

The traps EB3/ET3 appeared in all our In-doped samples except T37.2 and, as table 8 shows, traps similar to EB3/ET3 have been reported by several authors. As these traps with features similar to EB3/ET3 have been observed most often in In-doped samples, it is possible that they are related to In. However, measurements by Tomitori and co-workers [7] of the concentration profiles for these traps in the vicinity of surfaces at which the stoichiometry of the material had been changed, have suggested that these traps may be associated either with cadmium interstitials or tellurium vacancies. The traps EB4/ET4 were seen in all undoped samples and also in one of the doped samples (T37.2) but similar DLTS-derived trap characteristics have been reported only in the case of epitaxial layers [3, 21]. The appearance of these traps in both our Bridgman and THM material and their persistence in samples annealed in liquid Cd suggest that they are more likely to involve native defects rather than residual impurities although neither can be ruled out. As noted earlier, the double ionization level for interstitial Cd is thought to be in the region E_c–(0.2–0.24) eV but the capture cross-section for the feature EB4/ET4 appears to be smaller than would be expected for such a centre.

Traps similar to EB5 observed in this study have been reported in other studies using the DLTS technique [6, 8, 21] as well as other techniques [30, 31]. Although they appeared only in Bridgman material in the present study, table 8 indicates that they have been observed in THM samples [8] and also in layers deposited by hot-wall epitaxy [21]. However, it is significant that these traps were not found in Bridgman-grown material which had been annealed in Cd liquid. Thus it seems that the trap EB5 may be related to a residual impurity, as was suggested by Ido *et al* [8] for their corresponding traps NA5/A6. Similarly, traps ET5 which were observed in the THM grown samples annealed in Cd-vapour but not in Cd-liquid fired samples are probably associated with impurities which, in our work, must have entered the material during the THM processing stage. Of course, it should be noted that the impurites may exist in association with native defects, to form complex centres. The existence of such complex states has been shown to account for the linear proportionality between the corresponding trap density, N_T and the free carrier concentration n observed in GaP [32] and CdS [33]. For trap ET5, the defect densities for the 3 samples in table 5 are seen to vary by approximately one order of magnitude, matching, almost exactly the one order of magnitude variation in free carrier concentration indicated in table 3. Thus, it seems reasonable to assume that these traps are due to native defect–impurity complexes.

As noted previously, the traps EB6/ET6 were observed in all the samples examined during this study, irrespective of doping or annealing conditions employed, and table 8 indicates that similar features have been reported in a variety of differently prepared materials. Several possibilities have been suggested for the origin of these levels including V_{Cd} or donor–V_{Cd} associate centres [3]. However, although a number of traps in the region E_c–(0.6–0.7) eV were commonly reported in earlier studies [1, 26, 34–40] to be associated with the V_{Cd}^{-} centre, the capture cross-section for EB6/ET6 seems to be too large for this. Furthermore, the data in tables 4 and 5 indicate an increase in trap density for longer annealing times in Cd suggesting that the corresponding defects are more likely to involve an excess of Cd rather than a deficit, supporting the suggestion by Takebe and co-workers [4, 23] that Cd_i centres are involved. Attention should also be given to the possibility that macroscopic defects are responsible. It is well known that precipitates of the constituents of the compound can be present in CdTe depending on

the growth conditions and the levels at 0.72 eV reported by Gelsdorf and Schroter [26] were shown to be associated with dislocations introduced by forming indentations in the sample close to the Schottky contact, but in this case, no capture cross-sections were reported.

Finally, the tap EB7/ET7 were not only found in all the samples studied but they were also the dominant feature in all these samples. Table 8 shows that similar very deep levels have been widely observed although the correspondence between the defect parameters listed in the table and those for EB7/ET7 is generally rather poor. One reason for this could be that this DLTS peak is a relatively broad feature and could result from more than one defect. Further work using samples with higher purity and better crystal quality will be needed to resolve this problem.

5. Summary and conclusions

The use of DLTS in this study has revealed the presence of eleven separate traps with activation energies ranging from 0.2 to 0.86 eV. Two of these (ET1 and EB3/ET3) could be related to the presence of In and similar traps have been observed by several other authors particularly in In-doped material. Three traps (EB1, ET5 and EB5) were considered to be associated with residual impurities as these could be removed by annealing in liquid cadmium. Three other traps (EB4/ET4, EB6/ET6 and EB7/ET7) were found to be common to both Bridgman and THM grown samples and could not be removed by the liquid cadmium annealing treatment so that the involvement of native defects is suspected. However, while this investigation has provided some very useful indicators concerning the structure of electrically active defects in materials prepared in different ways it is clear that before definitive assignments can be made, greater control will need to be exerted over the residual impurity content and crystal quality of the materials under study. Fortunately, with the improving availability of high-quality material produced by means of low-temperature growth techniques such as molecular beam epitaxy, the development of an improved understanding of the defects in CdTe and related materials should be facilitated and work on such materials is now in progress in this laboratory.

References

[1] deNobel D 1959 *Philips Res. Rep.* **14** 361
[2] Kroger F A 1965 *J. Phys. Chem. Solids* **26** 1707
[3] Sitter H, Heinrich H, Lischka K and Lopez-Otero A 1982 *J. Appl. Phys.* **53** 4948
[4] Takebe T, Hirate T, Savaie J and Matsunami H 1982 *J. Phys. Chem. Solids* **43** 5
[5] Collins R T, Kuech T F and McGill T C 1982 *J. Vac. Sci. Technol.* **21** 191
[6] Isett L C and Reychaudhuri P K 1984 *J. Appl. Phys.* **55** 3605
[7] Tomitori M, Ishii S, Kuriki M and Hayakawa S 1985 *Japan J. Appl. Phys.* **24** 1488
[8] Ido T, Heurtel A, Triboulet R and Y-Marfaing 1987 *J. Phys. Chem. Solids* **48** 781
[9] Verity D, Shaw D, Bryant F J and Scott C G 1982 *J. Phys. C: Solid State Phys.* **15** L573
[10] Van der Pauw J L 1958 *Philips Res. Rep.* **13** 1
[11] Lang D V 1974 *J. Appl. Phys.* **45** 3023
[12] Guldberg J 1977 *J. Phys. E: Sci. Instrum.* **10** 1016
[13] Lang D V and Logan R A 1974 *J. Electron. Mater.* **14** 1053
[14] Lang D V 1979 *Thermally Stimulated Relaxation in Solids* ed E P Braunlich (Berlin: Springer) ch 3
[15] Miller G L, Lang D V and Kimerling L C 1977 *Ann. Rev. Mater. Sci.* **7** 377

[16] Aven M and Woodbury H H 1962 *Appl. Phys. Lett.* **1** 53
[17] Smith F T J 1970 *Metall. Trans.* **1** 617
[18] Hussein M, Lleti G, Sagnes G, Bastide G and Rouzeyre M 1981 *J. Appl. Phys.* **52** 261
[19] Verity D, Shaw D, Bryant F J and Scott C G 1983 *Phys. Status Solidi* a **78** 267
[20] Verity D, Shaw D, Bryant F J and Scott C G 1982 *J. Cryst. Growth* **59** 234
[21] As D J and Palmetshofer L 1985 *J. Cryst. Growth* **72** 246
[22] Tomitori M, Kuriko M, Ishii S, Fuyki S and Hayakawa S 1985 *Japan J. Appl. Phys.* **24** L239
[23] Takebe T, Sayaie J and Matsunami H 1982 *J. Appl. Phys.* **53** 457
[24] Triboulet R, Legros R, Heutel A, Sieber B, Dider G and Imhoff D 1985 *J. Cryst. Growth* **72** 90
[25] Lee W I, Takay N R, Bhat I B, Borrego J M and Ghandhi S K 1987 19th IEEE Photovoltaic Specialist Conf. (New York: IEEE)
[26] Gelsdorf F and Schroter W 1984 *Phil. Mag.* A **49** L36
[27] Whelan R C and Shaw D 1968 *Phys. Status Solidi* **29** 145
[28] Rud Yu V and Sanin K V 1971 *Sov. Phys.–Semicond.* **5** 244
[29] Zayachkivskii V P and Matlak V V 1974 *Sov. Phys.–Semicond.* **8** 675
[30] Zanio K 1978 *Semiconductors and Semimetals* vol 13 (New York: Academic) p 164
[31] Kroger F A 1977 *Rev. Phys. Appl.* **12** 205
[32] Krispin P 1982 *Phys. Status Solidi* a **69** 193
[33] Verity D, Shaw D, Bryant F J and Scott C G 1983 *Phys. Status Solidi* a **78** 267
[34] Scharger C, Uller J C, Stuck R and Siffer P 1975 *Phys. Status Solidi* a **31** 247
[35] Cuperlik R, Kargerova J and Klier E 1969 *Czech. J. Phys.* B **19** 1003
[36] Lorenz M R and Segall B 1963 *Phys. Lett.* **7** 18
[37] Agrinskaya N V, Arkad'eva E M, Matveeev O A and Rud'yu V 1969 *Sov. Phys.–Semicond.* **1** 776
[38] Chapnin V A 1969 *Sov. Phys.–Semicond.* **3** 481
[39] Sokolova V A, Vavilov V S, Plotonikov A F and Chapnin V A 1969 *Sov. Phys.–Semicond.* **3** 612
[40] Vul B. M., Vavilov V S, Ivanov V S, Stofachinskii V B and Chapnin V A 1973 *Sov. Phys.–Semicond.* **6** 1255